SAND REPORT
SAND2003-3818
Unlimited Release
Printed November 2003

Nanostructured Polyoxometalate Arrays with Unprecedented Properties and Functions

May Nyman, Darren Dunphy, Seema Singh, and C. Jeffery Brinker

Prepared by
Sandia National Laboratories
Albuquerque, New Mexico 87185 and Livermore, California 94550

Sandia is a multiprogram laboratory operated by Sandia Corporation, a Lockheed Martin Company, for the United States Department of Energy under Contract DE-AC04-94AL85000.

Sandia National Laboratories

Issued by Sandia National Laboratories, operated for the United States Department of Energy by Sandia Corporation.

Available to DOE and DOE contractors from
U.S. Department of Energy
Office of Scientific and Technical Information
P.O. Box 62
Oak Ridge, TN 37831

Telephone: (865)576-8401
Facsimile: (865)576-5728
E-Mail: reports@adonis.osti.gov
Online ordering: http://www.doe.gov/bridge

Available to the public from
U.S. Department of Commerce
National Technical Information Service
5285 Port Royal Rd
Springfield, VA 22161

Telephone: (800)553-6847
Facsimile: (703)605-6900
E-Mail: orders@ntis.fedworld.gov
Online order: http://www.ntis.gov/help/ordermethods.asp?loc=7-4-0#online

SAND2003-3818
Unlimited Release
Printed November 2003

Nanostructured Polyoxometalate Arrays with Unprecedented Properties and Functions

May Nyman
Geochemistry Department

Darren Dunphy
Chemical Synthesis and Nanomaterials

Seema Singh
Chemical Synthesis and Nanomaterials

C. Jeffery Brinker
Chemical Synthesis and Nanomaterials

Sandia National Laboratories
P.O. Box 5800
Albuquerque, New Mexico 87185

Abstract

Polyoxometalates (POMs) are ionic (usually anionic) metal –oxo clusters that are both functional entities for a variety of applications, as well as structural units that can be used as building blocks if reacted under appropriate conditions. This is a powerful combination in that functionality can be built into materials, or doped into matrices. Additionally, by assembling functional POMs in ordered materials, new collective behaviors may be realized. Further, the vast variety of POM geometries, compositions and charges that are achievable gives this system a high degree of tuneability. Processing conditions to link together POMs to build materials offer another vector of control, thus providing infinite possibilities of materials that can be nano-engineered through POM building blocks. POM applications that can be built into POM-based materials include catalysis, electro-optic and electro-chromic, anti-viral, metal binding, and protein binding. We have begun to explore three approaches in developing this field of functional, nano-engineered POM-based materials; and this report summarizes the work carried out for these approaches to date. The three strategies are: 1) doping POMs into silica matrices using sol-gel science, 2) forming POM-surfactant arrays and metal-POM-surfactant arrays, 3) using aerosol-spray pyrolysis of the POM-surfactant arrays to superimpose hierarchical architecture by self-assembly during aerosol-processing. Doping POMs into silica matrices was successful, but the POMs were partially degraded upon attempts to remove the structure-directing templates. The POM-surfactant and metal-POM-surfactant arrays approach was highly successful and holds much promise as a novel approach to nano-engineering new materials from structural and functional POM building blocks, as well as forming metastable or unusual POM geometries that may not be obtained by other synthetic methods. The aerosol-assisted self assembly approach is in very preliminary state of investigation, but also shows promise in that structured materials were formed; where the structure was altered by aerosol processing. We will be seeking alternative funding to continue investigating the second synthetic strategy that we have begun to develop during this 1-year project.

Acknowledgments

This work was supported by Sandia's Laboratory Directed Research and Development (LDRD) Project 52746. Sandia is a multiprogram laboratory operated by Sandia Corporation, a Lockheed Martin Company, for the United States Department of Energy under Contract DE-AC04-94AL85000.

CONTENTS

Figures

Tables

This page intentionally left blank

Executive Summary

The aim of this work is to develop materials with unprecedented forms and functions, using polyoxometalate (POM) clusters both as functional building blocks and functional "dopants". Some exploitable properties of POM clusters include electro-optic and electro-chromic response, pathogen/protein binding, metal binding, and catalysis. By incorporating POMs into organized arrays and robust materials while maintaining their functionalities, we aim to realize unprecedented properties including collective electro-optic response, and pathogen filtration/mitigation/detection. While bulk electro-optic behavior is well known, collective electro-optic behavior of POM arrays is still poorly understood. While virus binding of POMs in solution has been recognized, pathogen attachment to a POM surface has not been achieved. Three synthetic strategies are being optimized and tuned for control over material structure (i.e. 1-d, 2-d or 3-d arrays) and function (i.e. electro-optic, pathogen sequestration, etc.). The synthetic strategies include: 1) POMs incorporated into silica-based porous materials, 2) POM-surfactant based arrays that can be further modified by reactions with functional (i.e. luminescent) or structural (linking) metals, and 3) aerosol processed precursor solutions of the materials listed above to impart unusual hierarchical structure on the POM-based materials, such as nested hollow spheres. Given the enormous diversity of available POM geometries, compositions, charges, sizes and shapes; we have the potential for a tightly tunable system in terms of architectural design and optimization of material functionality. By coupling the fine control of the POM properties with the variety of material assembly techniques for which we are rapidly gaining experience and expertise, we are approaching a materials class with infinite possibilities for new collective behaviors based on the bulk properties that the POMs bring to the system. We are also breaking ground for development of novel POM applications that require controlled assembly of functional species in robust materials.

This page intentionally left blank

List of Acronyms

Aqueous	aq
Atomic Force Microscopy	AFM
Cetyltrimethylammonium Bromide	CTAB
Ethylenediaminetetraacetic Acid	EDTA
Fourier Transform Infrared Spectroscopy	FTIR
Heteropolyanion	HPA
Infrared Spectroscopy	IR
Isopolyanion	IPA
Lanthanide or Rare Earth Metal	Ln
Metal	M
Nuclear Magnetic Resonance Spectroscopy	NMR
Polyoxometalate	POM
Precipitate	ppt
Silicomolybdic Acid	SMA
Surfactant	S
Transmission Electron Microscopy	TEM
Ultraviolet Visible Spectroscopy	UV/vis
X-ray Diffraction	XRD

This page intentionally left blank

1.0 Introduction

Polyoxometalates (POMs) are anionic metal-oxo clusters of the early d^0 transition metals (Mo, W, Nb, V, Ta) where these metals are octahedrally coordined.(Pope, 1983) Clusters usually consist of ~4 – 30 octahedra with negative charges ranging from around –3 to –20 (there are a few exceptionally larger POMs; but these are the exception rather than the norm). POMs are usually around 1 nm (or 10 Å in size). The octahedra are corner and edge-sharing; and POM clusters may or may not contain 'dopant' heteroatoms in the octahedral sites. POMs may also contain tetrahedral sites (often P, Si, Ge), forming a subclass of POMs referred to as heteropolyanions, or HPA. If the POMs contain no tetrahedral sites, they are called isopolyanions, or IPA. Given the range of POM composition, geometry, and possibilities for heteroatom substitutions, the diversity of POM types is immense. Two of the more common geometries, the Lindquist ion (isopolyanion) and the Keggin ion (heteropolyanion) are illustrated in **figure 1**. The redox chemistry, the electrochemistry, the acid-base chemistry, and the charge density of POMs render these materials highly exploitable for a variety of applications. Some applications that have been pursued include electrochromic and electro-optic behavior, (Sadakane and Steckhan, 1998; Yamase, 1998) virus and protein binding,(Rhule et al., 1998) metal binding (including radionuclides) (Katsoulis, 1998), catalysis,(Kozhevnikov, 1998; Mizuno and Misono, 1998) and building blocks for materials.(Coronado and Gomez-Garcia, 1998)

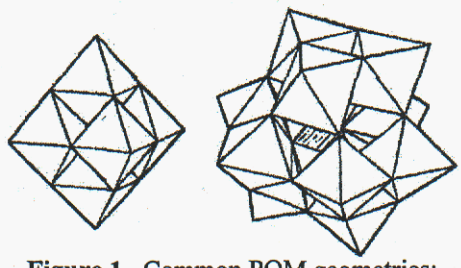

Figure 1. Common POM geometries: Left--lindquist ion $(M_6O_{19})^{x-}$; x=2-8 Right--Keggin ion $(TM_{12}O_{40})^{y-}$; y=3-16; M=octahedral metal, T-tetrahedral metal.

It is the POM application of material building blocks that we are predominantly pursuing in the work summarized in this report. We have investigated: 1) Incorporating POMs into silica-based matrices as dopants where the silica matrix has both micro- and meso-architecture, and 2) Developing a general procedure for using POMs as anionic subunits of POM-based materials. In the case of POM-doped, silica materials, the challenge is producing POM-doped materials in which the POMs retain their functionality (i.e. catalytic behavior) (Johnson and Stein, 2001; Maldotti et al., 2002; Moller and Bein, 1998; Okuhara, 2001). This is because to tether the POMs in a robust material, they must be chemically bound, which decreases the accessibility and the reactivity of the POMs. In particular, the metals, protons and oxygens that impart chemical and electrical activity to these clusters become less accessible and less reactive. In addition to doping microporous silica with POMs, we are interested in imparting hierarchical structure to obtain mesoporosity, or nested sphere structures. This was demonstrated by Brinker et al. using an aerosol spray technique, where self-assembly of nested sphere structures was induced by solvent evaporation.(Fan et al., 2001; Lu et al., 1999) Several applications were targeted by this approach to materials assembly. By incorporating optically active (i.e. luminescent) POMs into the mesostructures, we aim to obtain materials with bulk collective behavior. These types of spherical/layered materials may also be used as slow

release capsules for POMs, targeting the pharmaceutical industry,(Rhule et al., 1998; Wang et al., 2003) or binding/detection of pathogens in an aqueous medium.

Our second approach to structuring materials using POM-based chemistry is by utilizing POMs as the major building block, where the POMs are linked together around pore templates. Developing materials from POM building blocks has been investigating without the use of pore templates,(Coronado and Gomez-Garcia, 1998) but porous structures have not been successfully formed. Metal-oxo anionic monomers or clusters are extremely important in both the formation of natural materials (minerals; i.e. zeolites) and manmade materials (i.e. silica gels, synthetic oxides). These anionic species are precursors for aqueous routes to metal oxide-based materials, and the geometry, size and charge of these species is highly dependent on the solution conditions such as pH, ionic strength, and concentration. However, we have devised a general synthetic approach to anionic, POM building blocks that can be manipulated in non-aqueous solutions. By using POM precursors in non-aqueous media, we gain better control over the anionic building block, and thus we gain better control over the structure and properties of the metal oxide that is formed from the building block. Given the enormous diversity of POM geometries, we have access to greater degree of control of formation of complex, nano-structured materials by this non-aqueous route. Conversely, this non-aqueous synthetic approach provides us a means of accessing POM geometries that are not easily obtained due to their inherent instability or high solubility in aqueous solutions. Therefore, we also gain better control over the types of building blocks that can be utilized; and are able to obtain previously inaccessible cluster geometries.

Our strategy for non-aqueous synthesis of POM materials was to first replace the alkali counterions of POM salts with surfactants to obtain POM-surfactant ion pairs. This gives a POM precursor that is now soluble in solvent other than water, that do not affect the stability of the POM. Additionally, the POM can be further reacted with linking metals or function metals to build up a metal-oxo framework, while the surfactant serves to template pore formation. Alternatively, the POM may be bound to a functional metal prior to precipitating with a surfactant. Additionally, the POM-surfactant material can be dissolved and cast as an ordered film. This variety of POM-surfactant processing techniques is summarized in the schematic in **figure 2.** Finally, since the POM-surfactant materials are relatively insoluble in water, we can use this strategy to isolate cluster geometries that may be otherwise unattainable due to instability or high solubility.

The other interest we have in this POM-surfactant system is understanding how the surfactants and POMs assemble as a function of varying POM charge (thus varying POM:surfactant ratio). Insights gained from these investigations will provide insight into how such organically templated systems are ordered in nature, and how we can best gain control over ordering in such hybrid systems.

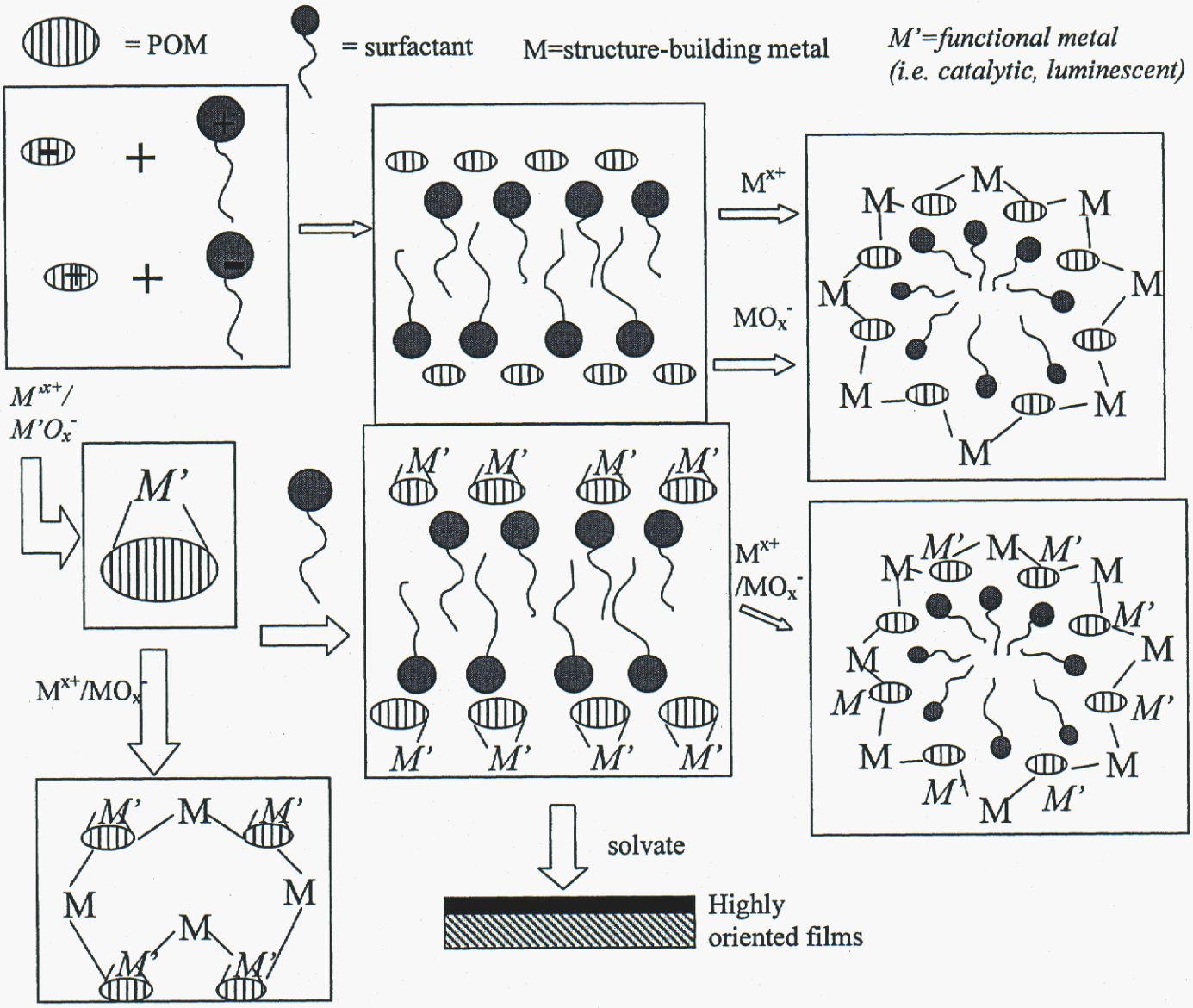

Figure 2. Synthetic 'Roadmap' to POM Arrays and POM-based Materials

2.0 Experimental

2.1 Synthesis of POM-doped Surfactant Templated Silica Films

A sol-gel route to porous surfactant-templated silica films doped with POMs was investigated. Because of the limited solubility in alcohol of the POMs used in this study (POMs **2** and **3** from **Table 1**), an aqueous silica sol recipe was developed that prevented precipitation of POM while limiting the silica condensation rate (a critical processing parameter for deposition of high-quality thin films). The non-ionic surfactant Brij® 56 (Aldrich tradename for polyoxyethylene(10) cetyl ether, $C_{16}H_{22}(OCH_2CH_2)_nOH$) was used as the pore template; unlike CTAB, Brij® 56 and POMs do not form insoluble ion pairs. Although the ratio of Brij® 56/silica was selected to form well-ordered 3D cubic pore structures, x-ray diffraction studies did not see any evidence of ordering at the POM/silica volume ratio studied (ca. 1:9). A typical sol recipe was 1 ml H_2O, 0.165 ml tetramethylorthosilicate (TMOS), 50 µL 1.0 N HCl, 62 mg Brij® 56, and 28 mg POM. Films were deposited onto silicon or quartz substrates using spin coating at 2000 rpm.
Three different strategies were employed to remove the surfactant template to leave a porous material; calcination in air at 350° for six hours, solvent extraction in a 1 N HCl ethanol solution for two hours at 80° C, or exposure to a short-wave UV lamp for two hours. The effects of these treatments on POM stability were studied using both transmission FTIR and UV/Vis spectroscopies.

2.2 Synthesis of POM-surfactant Arrays

The POM clusters that we have used thus far in our study are summarized in **Table 1**, along with the solvent in which the resultant POM-surfactant material is soluble. The general procedure for POM-surfactant synthesis is as follows. The POM (0.1 g) is dissolved in deionized water (10 – 30 ml) in one beaker by stirring, and heating if necessary. The surfactant (equal molar equivalents as the POM charge and number of charge-balancing cations) is dissolved in a second beaker of deionized water (10 – 30 ml), with heating. The surfactant used for this preliminary set of experiments is cetyltrimethylammonium bromide, $Br(CH_3)_3N^+\text{-}C_{16}H_{33}$; a C_{16}-chain length ammonium surfactant (commonly known as CTAB) for the anionic POMs. The surfactant for the cationic POM is sodium laurel sulfate, $NaSO_4^-\text{-}C_{12}H_{25}$. Note: the amount of water used to dissolve the POM and the surfactant is not so critical, since all the POM-CTAB materials have very low solubility in water. (However, this was not always the case for some short chain surfactant materials) The POM solution and the surfactant solution were then combined and immediately a flocculent formed, which was filtered and washed with warm water to remove any excess salts or surfactant. The yield was usually greater than 90%, and can be described as a creamy white to white, waxy solid. This reaction can be summarized as the following:

$$A_y(POM)^y\,(aq) + y(S\text{-}X)\,(aq) \rightarrow y(POM\text{-}S)\,(ppt) + AX \quad (1)$$

A = counterion for POM; y = charge on POM; S = surfactant; X = counterion for surfactant.

Table 1. Summary of POMs used for POM-Surfactant Synthesis

	POM formula	Formula weight	POM charge	Solvent for POM-surfactant*
1	$[AlO_4Al_{12}(OH)_{24}(H_2O)_{12}][SO_4^{-}\text{-}C_{12}H_{25}]_7$¶	2894	+7	butanol or butanol-water
2	$[PW_{12}O_{40}]H_3 \cdot xH_2O$	2880	-3	acetone or methylethylketone
3	$[SiMo_{12}O_{40}]H_4 \cdot xH_2O$	1823	-4	acetone or methylethylketone
4	$Na_7[HNb_6O_{19}] \cdot 15H_2O$	1294	-7	ethanol or ethanol-water
5	$Na_8[Ti_2Nb_8O_{28}] \cdot 34H_2O$	2084	-8	ethanol or ethanol-water
6	$K_8[SiW_{11}O_{39}] \cdot 13H_2O$	3223	-8	insoluble
7	$Na_{14}[H2Si4Nb_{16}O_{56}] \cdot 45.5H_2O$	3639	-14	pentanol or pentanol-water
8	$Na_{16}[SiNb_{12}O_{40}] \cdot 4H_2O$	2224	-16	pentanol or pentanol-water

**surfactant = CTAB with the exception of the cationic polyoxo-aluminate*

¶*this POM was formed directly with the surfactant without the intermediate step of salt formation*

2.3 Recrystallization of POM-surfactant Arrays

Attempts to recrystallize the POM surfactant arrays is work in progress. The purpose of this work is to obtain good quality crystals for single-crystal structure determination, so that we can understand how the different charge, geometry, and composition of the POMs affects how they interact with the surfactants in solid-state structures. Initially, we determined which POM-surfactant arrays were soluble in which solvents. Generally, alcohols and ketones were the best candidates, or alcohol-water and ketone-water mixtures.

In general, the greater the POM charge (thus more charge-balancing surfactants per POM), the longer chain alcohol required for dissolution. Two methods were used for recrystallization. In the first method, a solution of the POM-surfactant was prepared in the appropriate solvent with stirring and heating; followed by filtration of undissolved matter if necessary. This solution was placed in a vial so that at least half the vial was empty. The vial was then placed in a larger vial containing methanol, and capped. Slow diffusion of methanol into the POM-surfactant solution resulted in slow crystallization of the POM-surfactant material. These experiments were done generally on the size scale of ~10-20 ml POM-surfactant solutions. For the second method for recrystallization, the POM surfactant was combined with the appropriate solvent mixture in excess of its solubility. This mixture was then placed in a thick-walled pyrex tube and sealed under vacuum. The pyrex tube was placed in a heated silicon oil bath and heated for up to a week. Recrystallization took place by continuous dissolution and precipitation of the POM-surfactant mixture. Thus far, the best quality crystals were obtained from **2** and **3** (see **Table 1**).

2.4 Synthesis of Metal-POM-surfactant Arrays

In these preliminary experiments, first a cationic metal was bound to the anionic POM, and then the metal-POM was precipitated with the appropriate amount of surfactant. The general reaction can be described as the following:

$$(POM)^{y-}(aq) + M^{z+}(aq) \rightarrow (M\text{-}POM)^{-y+z}(aq) \qquad (2)$$

$$(M\text{-}POM)^{-y+z}(aq) + y\text{-}zS\,(aq) \rightarrow \textbf{M-POM-S}\,(ppt) \qquad (3)$$

y = charge on POM; S = surfactant; z = charge on metal; **M-POM-S** = metal-POM-surfactant precipitate

We carried out a few of these experiments to begin to develop robust structural materials and functional materials from the POM-surfactant arrays. The POMs used for these studies included $K_8[SiW_{11}O_{39}]\cdot 13H_2O$ (**6**) and $Na_{16}[SiNb_{12}O_{40}]\cdot 4H_2O$ (**8**); and the metals used included Fe^{3+}, Ce^{3+}, Yb^{3+} and Eu^{3+}. Lanthanides were initially investigated for interest in luminescent materials. The particular lanthanides that were investigated were chosen to give a range of cationic size where Ce^{3+} (1.15Å) > Eu^{3+} (1.09Å) > Yb^{3+} (1.01Å) for six-coordinate species. Both POMs, (**6**) and (**8**) were chosen for their potential superior metal-binding capabilities: (**6**) is a silicotungstate lacunary (meaning incomplete--a monovacant lacunary cluster is minus one M-O unit, thus providing a pocket for metal binding). POM and has known metal-binding behavior and (**8**) has a high ionic charge which should be conducive to good metal binding behavior. In the case of metal-binding with (**8**), the metal (Ce^{3+}) first had to be stabilized in a basic solution to prevent precipitation of cerium hydroxide upon contact with the basic solution of (**8**), which was achieved using a chelating reagent, EDTA and is detailed below.

2.4.1 Ce^{3+}-$[SiNb_{12}O_{40}]^{16-}$-CTAB synthesis

In 10 ml deionized water, ~25 drops of 1 M NaOH solution was added. 0.13 grams of Na_2H_2[EDTA] (disodium ethylenediaminetetraacetic acid) was dissolved in the basic solution. Cerium nitrate hexahydrate (0.15 g) was then dissolved in a minimal amount of water (~1 ml) and added to the [EDTA] solution. The resultant solution was clear, pale yellow with a pH around 11. 0.1 gram of $Na_{16}[SiNb_{12}O_{40}]\cdot 4H_2O$ POM was then dissolved in 10 ml of water. The Ce-[EDTA] solution (1.3 g of solution) was then added dropwise to the POM solution. A clear, bright yellow solution was obtained. The bright yellow color was indicative of binding of the POM to the Ce^{3+}. CTAB (0.2 g) was dissolved in 5 mL of water and added dropwise to the bright yellow solution. A bright yellow, glassy flocculent was obtained and isolated by filtration.

2.4.2 Ln^{3+}-$[SiW_{11}O_{39}]^{8-}$-CTAB synthesis (Ln = Ce, Yb, Eu)

$K_8[SiW_{11}O_{39}]\cdot 13H_2O$ (**6**) POM (0.2 grams, 0.062 mmol) was dissolved in 10 ml of water. An equimolar amount of the lanthanide salt was dissolved in 5 ml of water (0.027 g of cerium nitrate hexahydrate, 0.023 g of europium chloride hexahydrate, and 0.024 g of ytterbium chloride, anhydrous). The lanthanide salt solution was added to the POM solution to form a clear solution. The Ce-solution turned orange, the Eu- and Yb-solutions remained colorless. Five molar equivalents (3.1 moles, 0.11 g) of CTAB was

dissolved in 5 ml of water and added to the metal-POM solution. In each case, a flocculent formed and was collected by filtration.

2.5 Characterization of POM-surfactant and metal-POM-Surfactant Materials

The POM-surfactant and metal-POM-surfactant materials were characterized by a number of spectroscopic methods. Structure was investigated by X-ray powder diffraction (XRPD) and transmission electron microscopy (TEM), preservation of the POM structure was investigated by infrared (IR) spectroscopy or ^{27}Al Nuclear Magnetic Resonance (NMR) (in the case of the polyoxo-aluminate). The solution ^{27}Al NMR spectra were obtained from a 5mm probe Bruker 400 MHz instrument with Al resonating at 104.26 MHz. The $[AlO_4Al_{12}(OH)_{24}(H_2O)_{12}][SO_4^{-}\text{-}C_{12}H_{25}]_7$ powder was dissolved in butanol and peaks were referenced externally to a 1 molar aqueous solution of $AlCl_3$ (0 ppm).

2.6 Aerosol-Generation of $[Nb_6O_{19}][CTAB]_8$ Particles

As a first attempt of aerosol processing of the POM-surfactant materials for formation of materials with hierarchical structure, we use the $[Nb_6O_{19}][CTAB]_8$ complex. A solution of $[Nb_6O_{19}][CTAB]_8$ in ethanol (ca. 2g complex/60 ml solvent) was aspirated into a TSI Inc. Model 3076 Constant Output Atomizer to form an aerosol, which was subsequently dried by a ca. 3 second transport through a tube furnace heated to 150°. Initial particle collection was by entrapment in a 0.2 μm filter. Unfortunately, the resulting particles were soft enough to fill the pores of the filter material, clogging the system and creating a dangerous backpressure on the particle generating system. Particles were subsequently collected as an aqueous suspension by bubbling the output of the tube furnace through a flask of water, yielding a milky solution.

3.0 Results and Discussions

3.2 Characterization of POM-doped Surfactant Templated Silica Films

Figure 3 shows infrared (IR) spectra of pure silicomolybdic acid (POM **3** from **Table 1**), an untreated surfactant-templated silica film, and POM-doped films before and after the three different surfactant removal methods. Data from the C-H stretch region around 3000 cm^{-1} (not shown) clearly demonstrates that all three template-removal strategies are completely effective in removing surfactant. Interestingly, films not doped with any POM but subjected to the UV treatment showed no surfactant removal, indicating that the POM is acting as a photocatalyst during the template removal process. Examination of the IR data below 1000 cm^{-1}, however, clearly demonstrates that all three surfactant removal strategies are detrimental to the entrapped POM to some degree. After calcination, there is no discernable IR absorbance for silicomoybdic acid. Solvent extraction appears to remove most of the entrapped POM, but a small fraction (perhaps

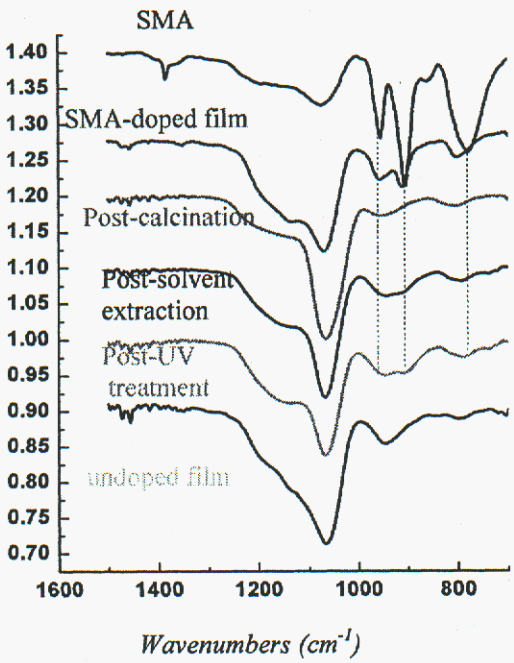

Figure 3. IR spectra of silicomolybdic acid doped films treated for template removal.

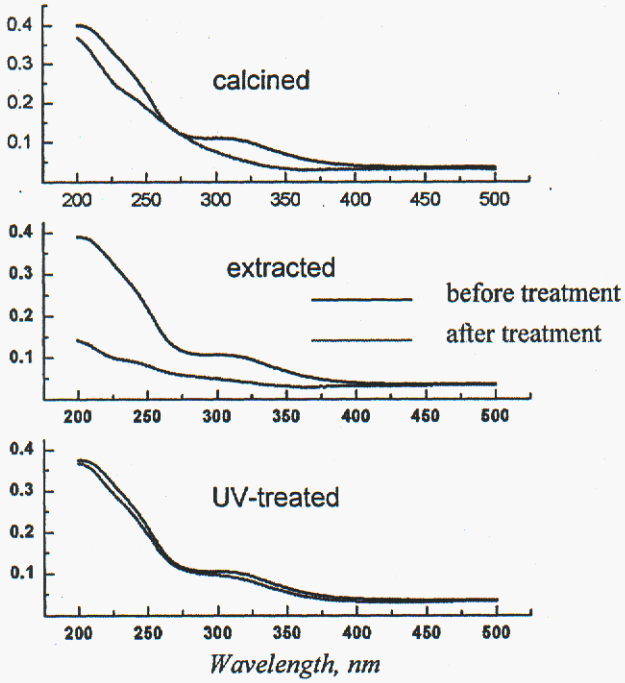

Figure 4. Effect of surfactant removal treatments of Brij® 56 templated films (doped with SMA).

located inside the silica walls) remains. For films treated with UV light the loss of POM integrity is much less than for the other two treatment routes, as indicated by the relative strength of the POM IR absorbance.

UV/Vis spectroscopy of films deposited on quartz substrates further confirms the results of the FTIR study. The data in **Figure 4** shows the POM electronic absorbance before and after the three different treatment methods. In calcined films, there is a significant shift in the shape of the absorbance spectrum, presumably due to the formation of molybdenum oxide from POM degradation. The absorbance spectrum for extracted films also appears to change shape while the absolute absorbance decreases by ca. 65%; it is likely that some POM degradation is occurring along with the removal of material by the extraction medium. Finally, although there is a small shift in the absorbance spectrum during UV treatment, the POM appears to be largely intact. The data for the other POM investigated, phosphotungstic acid (**2** from **Table 1**), is nearly identical to that of the data for silicomolybdic acid, showing the same general trends in POM stability during the three surfactant removal treatments.

3.3 Characterization of POM-surfactant arrays

3.2.1 Retention of POM structure in ordered arrays

In order to investigate applications of anionic POM-Surfactant arrays or further react the POM-Surfactant material for a variety of applications, the POMs must remain unaltered upon precipitation with the surfactant. This is shown to be the case by infrared (IR) spectroscopy. The spectrum in **figure 5** illustrates this for POM-S with

POM=$[SiNb_{12}O_{40}]^{16-}$ and S= CTAB. The red spectrum shows the parent POM, $Na_{16}[SiNb_{12}O_{40}]\cdot 4H_2O$. The POM vibrations are predominantly between 400 – 1000 cm^{-1}. The green spectrum is the surfactant, CTAB, for reference, and the blue spectrum is the POM-S, $[SiNb_{12}O_{40}][(CH_3)_3N^+\text{-}C_{16}H_{33}]_{16}$. **Figure 5** illustrates that the POM is not chemically altered by ordering with the surfactant: the POM-S spectrum is essentially the sum of the spectra of the CTAB and the POM. This was the case for all the POMs investigated, which suggests that this synthetic route is mild and generally useful for

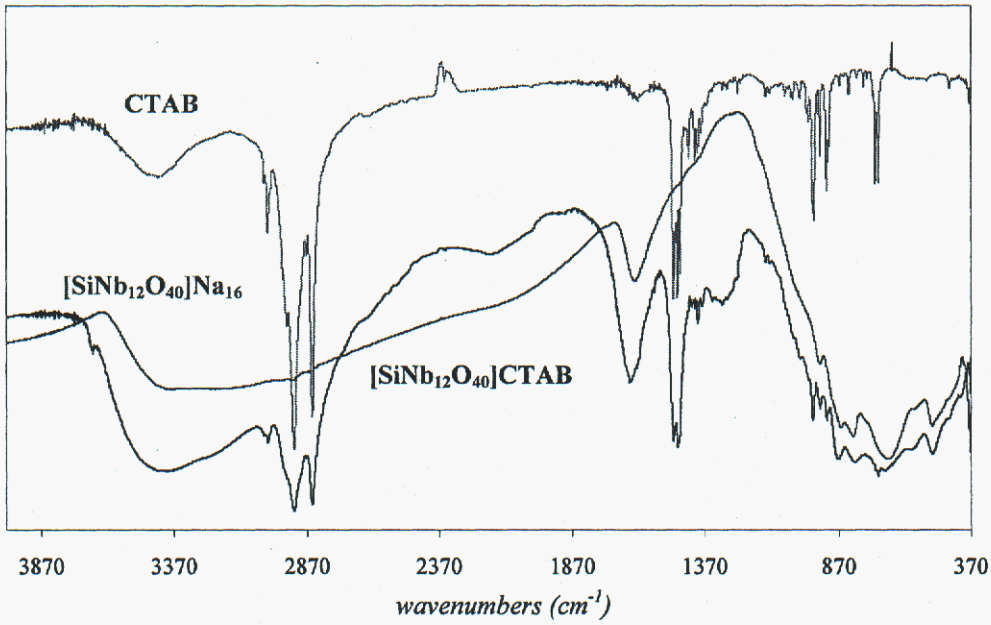

Figure 5. Infrared spectrum showing retention of the POM geometry upon Precipitation as a lamellar POM-surfactant material.

capturing a variety of POM geometries and compositions in a non-aqueous medium that can be used for further chemical reactivity.

While infrared spectroscopy was a good means to validate the nature of the POM cluster for the anionic POMs, it was not appropriate for the polyoxoaluminate (cluster 1 in Table 1) due to the inherent broad and featureless IR spectrum of this phase. Instead, ^{27}Al NMR was utilized. By ^{27}Al NMR a single peak at +63.6 ppm was observed which corresponds with the AlO_4 tetrahedral site.(Allouche et al., 2001) The twelve AlO_6 octahedral sites are not observable by NMR due to the quadrapolar broadening (spin 5/2) of this distorted site, which results in broadening of this peak into the spectrum baseline. Although in the case of an aqueous solution, the peak can be observed by heating, this was not possible in the butanol solvent.

3.3.2 Preliminary Characterization of POM-Surfactant ordering

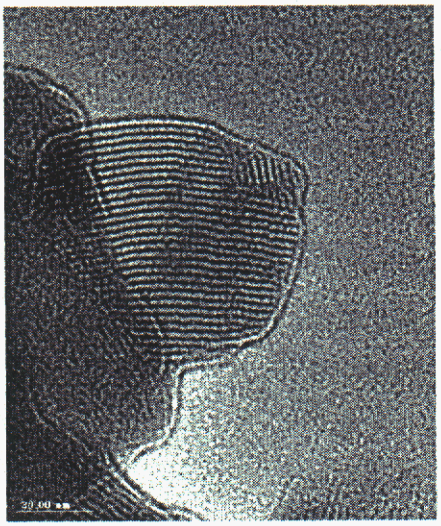

Figure 6. TEM image of $[H_2Si_4Nb_{16}O_{56}][(CH_3)_3N^+\text{-}C_{16}H_{33}]_{14}$, revealing the lamellar phase that dominates metal-surfactant products.

Characterization of the POM-S materials by powder X-ray diffraction and Transmission Electron Microscopy (TEM) reveals a predominant lamellar structure, in every case investigated thus far. **Table 2** lists the d-spacing of the (001) peaks of the different POM-S materials. In each case the surfactant is CTAB (with the exception of the polyoxocation, which is charge-balanced with laurylsulfate), and the diffraction pattern is obtained from a film spin-coated on a (001) mica surface from an alcohol or ketone solution. In general, the (001) d-spacing increases with increasing charge of the POM, which directly corresponds with increasing number of surfactants to charge-balance the POM. The exception is the $[SiMo_{12}O_{40}][(CH_3)_3N^+\text{-}C_{16}H_{33}]_4$. Its (001) d-spacing is considerably smaller than the rest of the POM-S materials we have made thus far. In fact it is even smaller than that of the CTAB. **Figure 6** shows a TEM image of $[H_2Si_4Nb_{16}O_{56}][(CH_3)_3N^+\text{-}C_{16}H_{33}]_{14}$, which is similar in appearance to all the POM-S materials by TEM. The lamellar structure is the dominant feature observed. A schematic of a possible structure of the inter-leaved arrangement of the surfactant chains with the POMs is shown in **figure 2**, where the negatively-charged ovals are the POMs and the positively charged circles with tails are the surfactants.

Table 2. POM-Surfactant (001) d-spacing

POM-surfactant composition	POM charge	d (001) Å *
$[[AlO_4Al_{12}(OH)_{24}(H_2O)_{12}][SO_4^-\text{-}C_{12}H_{25}]_7$	7+	35.8
$[PW_{12}O_{40}][(CH_3)_3N^+\text{-}C_{16}H_{33}]_3$	3-	30.2
$[SiMo_{12}O_{40}][(CH_3)_3N^+\text{-}C_{16}H_{33}]_4$	4-	22.8
$[HNb_6O_{19}][(CH_3)_3N^+\text{-}C_{16}H_{33}]_7$	7-	31.8
$[Ti_2Nb_8O_{28}][(CH_3)_3N^+\text{-}C_{16}H_{33}]_8$	8-	31.8
$[H2Si4Nb_{16}O_{56}]$ $[(CH_3)_3N^+\text{-}C_{16}H_{33}]_{14}$	14-	33.5
$[SiNb_{12}O_{40}][(CH_3)_3N^+\text{-}C_{16}H_{33}]_{16}$	16-	34.0

*d-spacing is referenced to the (001) spacing of mica, 9.96 Å

Although the X-ray diffraction data strongly suggest a predominant lamellar structure of the POM-S materials, it is difficult to understand how the POMs with different charges can arrange in the same manner. In other words, how can 16:1 S:POM ratio have the same structure as a 3:1 S:POM ratio? With ongoing work, we are trying to determine the answer to this question using a variety of characterization techniques including TEM,

atomic force microscopy (AFM), and perhaps some more specialized techniques such as surface neutron reflectivity. Electron diffraction patterns of $[SiNb_{12}O_{40}][(CH_3)_3N^+\text{-}C_{16}H_{33}]_{16}$ and $[Ti_2Nb_8O_{28}][(CH_3)_3N^+\text{-}C_{16}H_{33}]_8$ are shown in **figure 7**, clearly showing a periodic arrangement of species in both cases. However, the former suggests a cubic arrangement of the clusters while the latter suggests a hexagonal arrangement of the clusters in the 2-d plane perpendicular to (001). In fact, the electron diffraction patterns perpendicular to (001) looked dissimilar to each other; suggesting a charge/geometry/composition effect on arrangement of the anionic clusters within the basal plane.

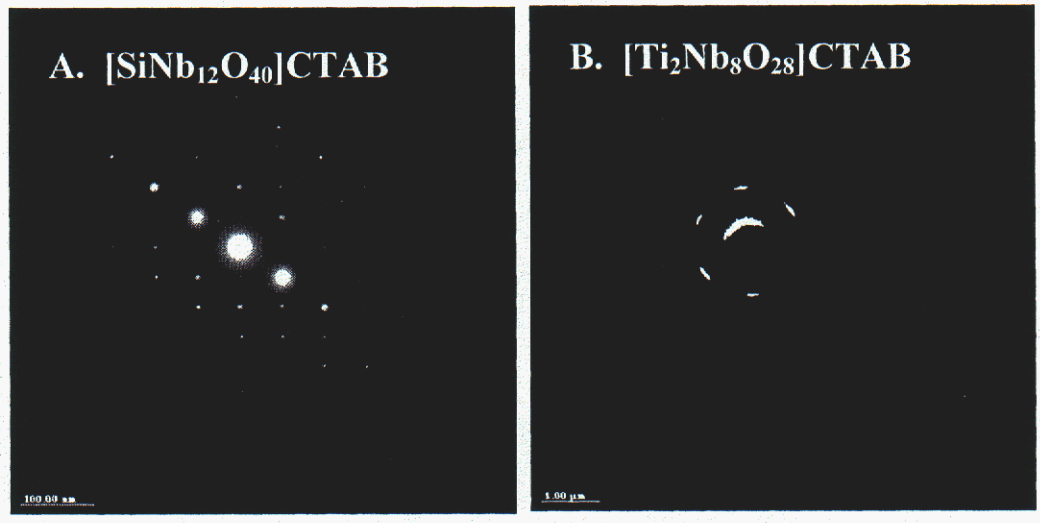

Figure 7. Electron diffraction images of two POM-surfactant phases showing the differing arrangement of anionic cluster species.

3.4 Characterization of Metal-POM-surfactant Materials

In the preliminary characterization of the materials formed by first binding a metal to a POM (either the $[PW_{11}O_{39}]^{8-}$ lacunary or the $[SiNb_{12}O_{40}]^{16-}$) followed by precipitation with a surfactant; these materials proved to be less well ordered than the POM-surfactant materials. This conclusion was postulated from the diffraction patterns (**figure 8**). While a broad (001) peak is evident at low angle (<3°), the peaks are broader and less intense than those of the POM-surfactant materials. The exception is the Ce-lacunary complex with a 2:1 ratio of the lacunary POM cluster to the Ce metal. The spectrum of this complex has a sharper and narrower peak and smaller (001) d-spacing than the 1:1 POM:Ce, POM:Eu and POM:Yb. The 2:1 reaction would give a $[SiW_{11}O_{39}]_2Ce^{13-}$ specie, whereas the 1:1 complex produces a $[SiW_{11}O_{39}]Ln^{5-}$ specie (Ln = Ce, Eu, Yb). This gives the opposite correlation as the POM-surfactant materials. That is; increasing POM complex charge corresponds with decreasing d-spacing. Clearly, this is only preliminary data and will be investigated further. One difficulty with these materials that frustrates further characterization is they have very poor solubility in the range of

solvents that have been tried thus far. However; to get around this problem, we plan to try different length surfactants which has proven to have significant influence over the solubility properties of the POM-surfactant or metal-POM-surfactant material.

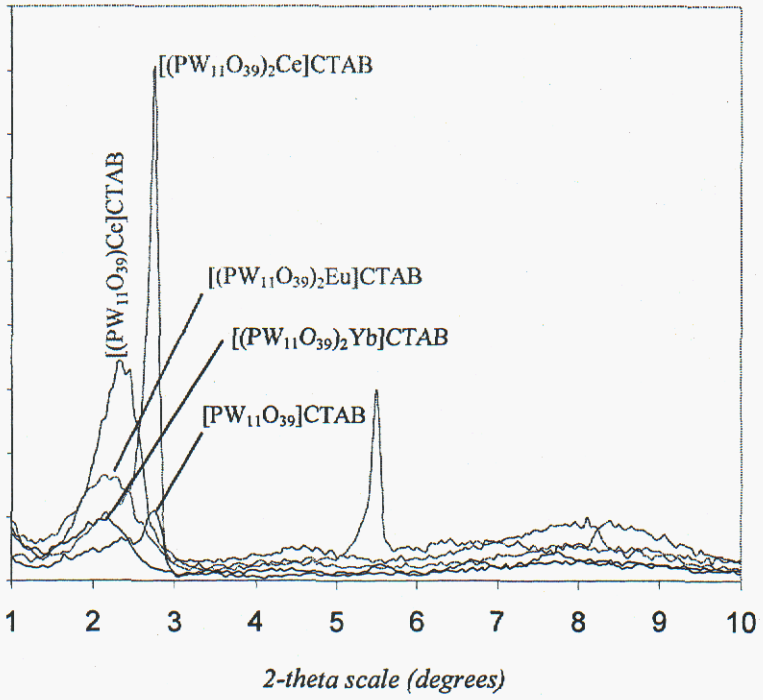

Figure 8. Low angle X-ray diffraction patterns of Metal-POM-surfactant materials.

Figure 9 compares the $[SiW_{11}O_{39}][CTAB]_8$ with the $Ce[SiW_{11}O_{39}]$-CTAB 1:1 complex to the $Ce[SiW_{11}O_{39}]_2$-CTAB 1:2 complex by infrared characterization. The spectra show sharp and well-resolved peaks, indicating the POM remains intact with no decomposition. The series of vibration peaks from around 600-1000 cm^{-1} are clearly directly related to bonding of the Ce atom to the vacant site of the lacunary complex, for these peak change from the parent compound to the 1:1 and 2:1 lacunary:Ce complexes.

Figure 10 shows the 1:1 lacunary POM:Ln complexes of Ce, Eu and Yb. These are quite similar to each other with slight differences on the small shoulder around 700 wavenumbers. This suggests that the mode of coordination of the lacunary ion with the lanthanides is quite similar, as we might expect since the chemistry of the lanthanides across the series does not vary significantly.

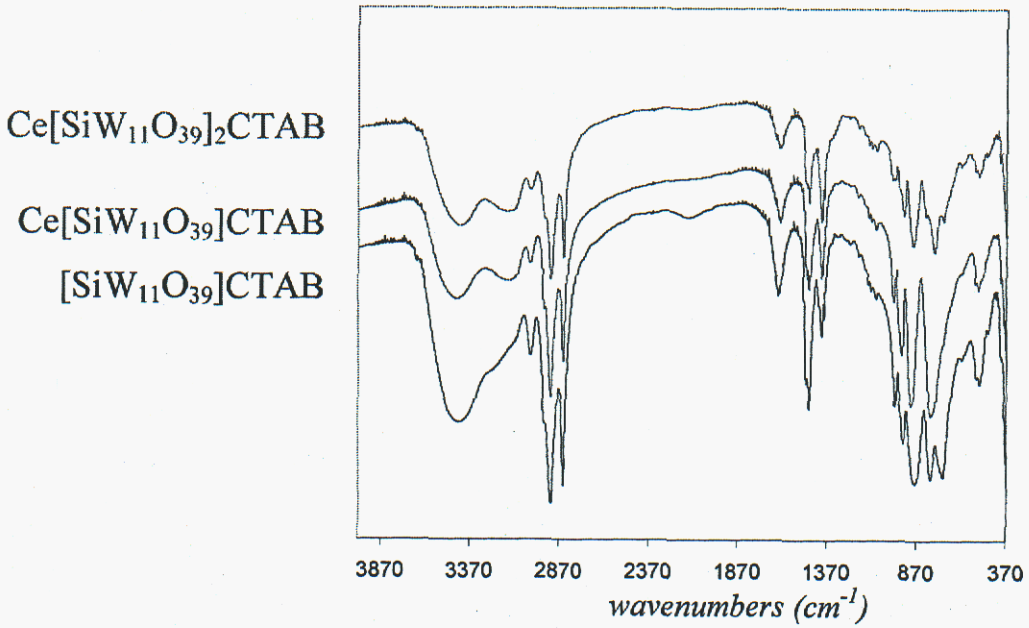

Figure 9. Infrared spectra of $[SiW_{11}O_{39}]CTAB$ and its Ce derivatives.

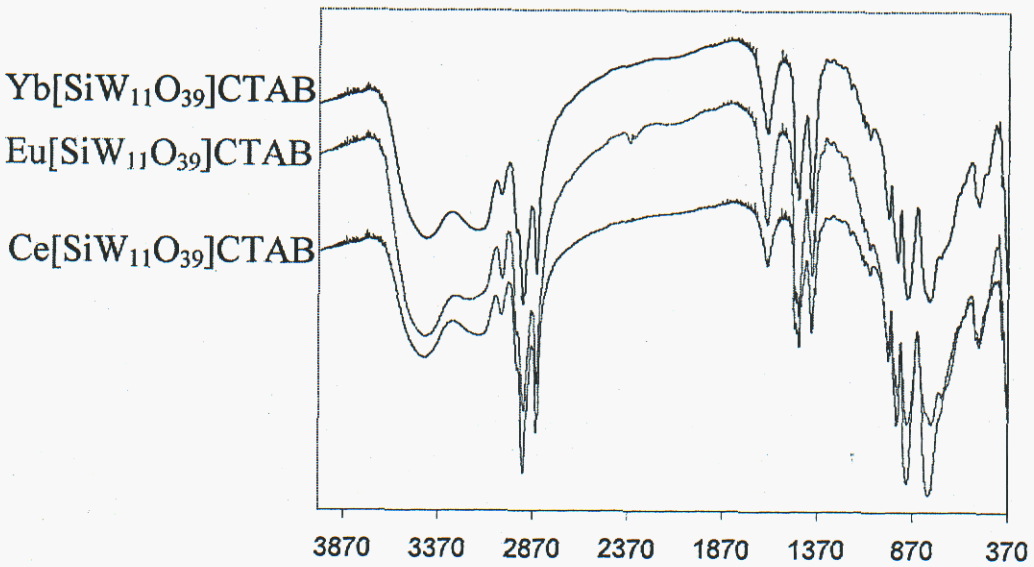

Figure 10. Infrared spectra of $Ln[SiW_{11}O_{39}]CTAB$ 1:1 derivatives.

3.5 Formation of ordered particles by evaporation-induced self assembly of an aerosol

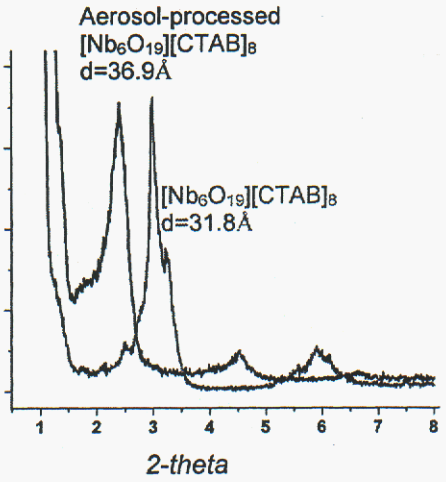

Figure 11. X-ray diffraction spectra comparing precipitated and aerosol-generated POM-surfactant arrays.

Ordered particles were formed by dissolving the POM/surfactant complex $[HNb_6O_{19}][CTAB]_8$ in ethanol and nebulizing this solution using an aerosol generator. Subsequent evaporation of solvent in this aerosol initiated self-assembly of particles with different mesoscale ordering than that seen in the parent complex before dissolution in alcohol. This was observed by X-ray diffraction characterization of the particles (**Figure 11**). The (001) d-spacing increases significantly from around 30 Å to 36 Å. Because the generated particles lacked the solidity needed for collection in a filter apparatus, particles were collected as a suspension in H_2O. Subsequent centrifugation of this suspension yielded a waxy substance made up of coagulated particles. Future work will focus on increasing the stability of these particles by addition of an outside layer of porous silica, creating a complex two-layer structure with novel properties.

4.0 Summary and Future Directions

The main goal of this 1-year out-of-the-box LDRD project was to develop a general synthetic procedure to synthesize POM-doped materials or POM-based materials that would incorporate the many useful properties of POM clusters into tailored functional materials. The three approaches we investigated include; 1) doping POMs into templated, silica matrices using sol-gel science, 2) developing metal-POM-surfactant arrays or POM-surfactant arrays as a basis for nano-structured POM-based materials, and 3) using aerosol-assisted spray pyrolysis to produce hierarchical structured materials. The first approach was hampered by inability to remove the templates and retain the POMs intact, as well as loss of self assembly upon addition of the POMs. The third approach has received only minimal attention thus far due to lack of equipment availability, but will be further pursued in parallel with the second approach. The second approach was the most successful, and many scientific questions and materials to be developed have grown out of this portion of the study. We will be following up on these issues with the general plans outlined below.

- *Understand how POM charge affects the architecture of POM-surfactant arrays.* We are achieving this goal by working on growing good quality crystals of the range of POM-surfactant materials in order to obtain complete structural analysis

from single-crystal X-ray data. With the POM-CTAB materials, we are investigating varying the temperature and solvent system for crystallization. We are also investigating the use of different surfactant chain lengths, which greatly changes the solubility behavior of the POM-surfactant material. Additionally, we are looking at the effect of POM charge on ordering POMs on a surface. This is being done by spin-casting POM-surfactant arrays on a flat surface such as mica and characterizing by atomic force microscopy (AFM).

- *Build 3-dimensional, ordered, POM-based materials using the POM-surfactants as "precursors".* The goal of this work is to develop the chemistry to link together POMs in ordered networks to build up 3-dimensional architectures. In these materials, we aim to retain the POM behavior including catalytic activity, acid-base chemistry, and electro-optical response. If appropriate, collaborations will be formed to characterize these behaviors. Additionally, we will build accessory material functionalities, such as by binding the POM to a luminescent metal (see section 3.4) prior to incorporating it into a structured, POM-based material. In this work we hope to not only develop POM-based materials in which POM functionalities are preserved, but to investigate the collective behavior of functional POMs that are assembled in interconnected array.
- *Use the surfactant-POM precipitation technique to capture and manipulate unprecedented or metastable POM geometries.* Many anionic clusters are known to exist in solution but are unattainable in the solid-state due to metastability or high solubility in the solution in which they are formed. By precipitating them as an ion pair with a surfactant, we then obtain a the POM in a form which it can handled in a less polar solvent in which it would be more stable. We will be aggressively seeking alternative or continued funding for this work.

5.0 References

Allouche L., Huguenard C., and Taulelle F. (2001) 3QMAS of Three Aluminum Polycations: Space Group Consistency Between NMR and XRD. *Jounal of Physics and Chemistry of Solids* **62**, 1525-1531.

Coronado E. and Gomez-Garcia C. J. (1998) Polyoxometallate-based Molecular Materials. *Chemical Reviews* **98**, 273-296.

Fan H., VanSwol F., Lu Y., and Brinker C. J. (2001) Multiphased Assembly of Nanoporous Silica Particle. *Journal of Non-Crystalline Solids* **285**, 71-78.

Johnson B. J. S. and Stein A. (2001) Surface Modification of Mesoporous, Macroporous and Amorphous Silica with Catalytically Active Polyoxometalate Cluster. *Inorganic Chemistry* **40**, 801-808.

Katsoulis D. E. (1998) A Survey of Applications of Polyoxometalates. *Chem. Rev.* **98**, 359-387.

Kozhevnikov I. V. (1998) Heteropoly Acids and Multicomponent Polyoxometalates Liquid-phase Reactions. *Chem. Rev.* **98**(1), 171-178.

Lu Y., Fan H., Stump A., Ward T. L., Rieker T., and Brinker C. J. (1999) Aerosol-assisted Self-assembly of Mesostructured Nanoparticles. *Nature* **398**(6724), 223-226.

Maldotti A., Molinari A., Varani G., Lenarda M., Storaro L., Bigi F., Maggi R., Mazzacani A., and Sartori G. (2002) Immobilization of $(n\text{-}Bu_4N)_4W_{10}O_{32}$ on Mesoporous MCM-41 and Amorphous Silicas for Photocatalytic Oxidation of Cycloalkanes with Molecular Oxygen. *Journal of Catalysis* **209**, 210-216.

Mizuno N. and Misono M. (1998) Heterogeneous catalysis. *Chem. Rev.* **98**(1), 199-217.

Moller K. and Bein T. (1998) Inclusion Chemistry in Periodic Mesoporous Hosts. *Chemistry of Materials* **10**, 2950-2963.

Okuhara T. (2001) Catalysis by Heteropoly Compounds--Recent developments. *Applied Catalysis A: General* **222**, 63-77.

Pope M. T. (1983) *Heteropoly and Isopoly Oxometalates*. Springer Verlag.

Rhule J. T., Hill C. L., and Judd D. A. (1998) Polyoxometallates in Medicine. *Chemical Reviews* **98**, 327-357.

Sadakane M. and Steckhan E. (1998) Electrochemical properties of Polyoxometalates as Electrocatalysts. *Chem. Rev.* **98**(1), 219-237.

Wang X., Liu J., and Pope M. T. (2003) New Polyoxometalate/Starch Nanomaterial: Synthesis, Characterization and Antitumoral Activity. *Dalton Transactions*, 957-960.

Yamase T. (1998) Photo and Electrochromism of Polyoxometalates and Related Materials. *Chem. Rev.* **98**(1), 307-325.

Distribution

MS 0323 D. L. Chavez, 1011
MS 0323 H. R. Westrich, 1011
MS 0511 C. E. Myers, 1010
MS 0750 May Nyman, 6118
MS 1349 C. J. Brinker, 1002
MS 1349 S. Singh
MS 1349 D. Dunphy, 1349
MS 9018 Central Tech. Files, 8945-1
MS 0899 Technical Library, 9616 (2)